ASPS Conference Proceedings 1: 1463-1469 (2022)

Proceedings of

12th Structural Engineering Convention-An International Event (SEC 2022)

Available at https://asps-journals.com/index.php/acp

Wind Interference Effect of Neighbouring Square Buildings in Rhombic Arrangement on an Octagonal Building

R. Kar [1,*] , S.K. Dalui [2]

[1] Department of Civil Engineering, Research Scholar, Indian Institute of Engineering Science and Technology, Shibpur, India
[2] Department of Civil Engineering, Assistant Professor, Indian Institute of Engineering Science and Technology, Shibpur, India

Paper ID - 140163

Abstract

Four square plan shaped tall buildings of the same height and lateral dimension are positioned at the vertices of a rhombus. The octagonal plan shaped tall building of same height is placed at the centroid of the rhombus. The wind-induced responses of the octagonal plan shaped tall building for specified interference cases are compared with that of the isolated cases. The octagonal plan shaped principal building is exposed to atmospheric boundary layer wind flow. The wind angle varies from 0° to 90° at an interval of 15° for both isolated and interfering conditions. Computational fluid dynamics is implemented to simulate the effect of wind-structure interaction on the principal and neighbouring buildings in the boundary layer wind flow. The wind-induced static responses like drag and lift coefficients, pressure coefficients for isolated and interference cases are evaluated and compared graphically. The responses of isolated and interference cases vary significantly with the varying wind incidence angle. The dynamic behaviour of wind is also thoroughly investigated to identify the adverse local effect on the different faces of the octagonal building. As the characterisation of wind-induced dynamic responses, peak pressure coefficients and power spectral densities are evaluated and plotted accordingly. The peak pressure coefficients are plotted against mean pressure coefficients. The power spectral densities for different interfering cases are compared with the isolated case. Significant variation in power spectral densities is observed in some cases, which portrays the different characteristics for formation and shedding of the vortices in the wake of the octagonal building. The comparison of various dynamic responses between isolated and interfering cases highlights the interference by the square plan shaped buildings.

Keywords: Computational fluid dynamics, Force Coefficient, Peak Pressure, Pressure Coefficient, Power Spectral Density

1. Introduction

The design of high-rise buildings needs to incorporate detailed wind-induced responses. The past investigations by the researchers mostly contain the analysis of wind loads on different plan shaped tall buildings either in stand-alone or interference condition. Sharma et al. (2019) investigated wind-induced responses of tapered and set-back structures. Sy et al. (2019) conducted static and dynamic interference tests in a wind tunnel to examine the detailed characteristics of wind over top flow among square plan shaped tall buildings. The effect of the various aerodynamic modification mechanisms on the dynamic behaviour of the principal building is explored (Lo et al., 2016; Lo and Kim, 2019) in the presence of a very closely located interfering building. Yu et al. (2015) studied interference effects on wind pressure distributions between two buildings with various configurations in tandem, oblique, and parallel arrangements. The analysis of the interference effects between two high-rise buildings with square and rectangular shapes has been carried out (Hui et al., 2012; Hui et al., 2013) by wind tunnel experiments, concentrating on local peak pressure coefficients. Yu et al. (2018) studied wind-induced interference effects on the along-wind and across-wind acceleration responses between two tall buildings with different section size.

A few studies have been conducted on octagonal plan shaped building with interference effect (Kar and Dalui, 2016; Kar et al., 2019). The present study is an important step in that direction. In the current study, the interference effect on an octagonal plan shaped tall building is inspected in the presence of four numbers of square plan shaped buildings in the rhombic pattern.

2. Problem formulation and Methodology

The actual height and section width of the octagonal plan shaped building is 150 m and 30 m respectively. The four numbers of square plan shaped buildings are placed around the principal building in a rhombic pattern, as shown in Fig. 1. The section dimension and height of the interfering buildings are the same as the principal building. The wind angle varies from 0° to 90° with an interval of 15°. The building setup is analysed by computational fluid dynamics (CFD) using ANSYS CFX.

*Corresponding author. Tel: +919432371195; E-mail address: ronykar123@gmail.com

Published online: December 19, 2022
doi:10.38208/acp.v1.677

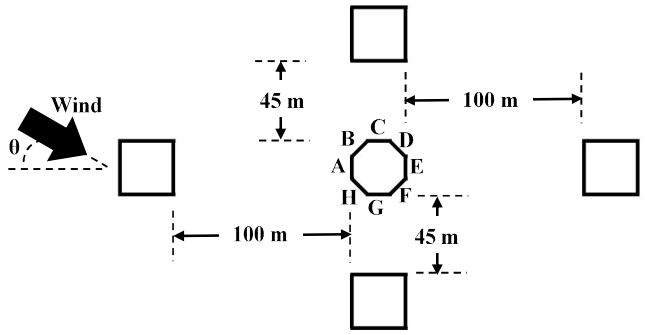

Fig. 1 Building setup for a typical interfering case

The freestream wind velocity is taken as 50 m/s. The wind profile is generated by the power law equation (Kar and Dalui, 2016) with an exponent of 0.133. The Shear Stress Transport (SST) turbulence model (Menter, 1994) is used to numerically simulate the boundary conditions of the wind flow.

3. Construction and discretisation of the computational domain

The computational domain for CFD analysis is constructed [9] as shown in Fig. 2. The discretisation of the domain is carried out using tetrahedral elements. The plan view of meshing for a typical interference setup is depicted in Fig. 3.

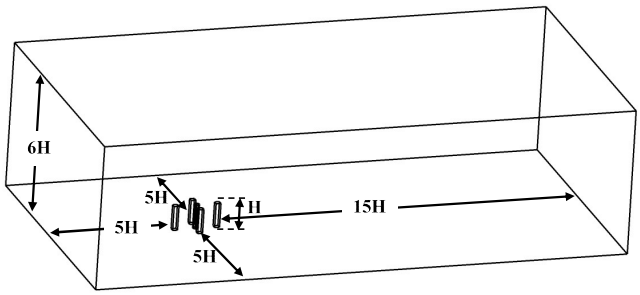

Fig. 2 The computational domain for typical interfering case

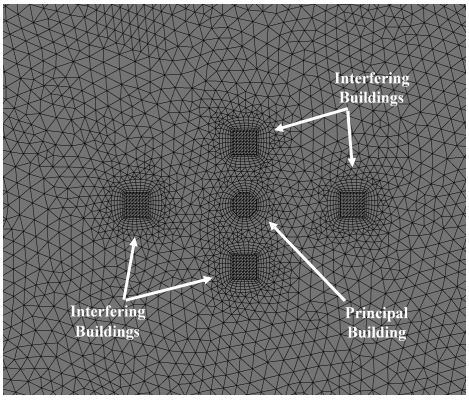

Fig. 3 The meshing for a typical interfering case

Table-1. Grid sensitivity study for interfering case

Sl. No	No. of elements	Force Coefficient	Error (%)
1	562916	0.6069	30.5
2	2426934	0.5542	19.2
3	8428010	0.4933	6.1
4	16707859	0.4684	0.7
5	39061729	0.4663	0.3
6	65375576	0.4650	-

3.1 Grid Sensitivity Study

A grid sensitivity study has been carried out to find out the optimum mesh density for the CFD analysis. The building setup in the interfering condition is subjected to 0° wind incidence angle and simulation is performed for increasing mesh density. The force coefficient for each case is compared and arranged in Table-1. It can be seen that with increasing mesh density, the error in the force coefficient decreases until the optimal mesh density is reached. Here, meshing density corresponding to case number 5 has been chosen as the representative mesh density, which is used for discretising all the other cases.

4. Results and Discussion

The interfering building setup is analysed for different wind incidence angles, and the responses are compared against the isolated case. Fig. 4 illustrates the flow pattern near the building setup at 0° wind angle. The faces A, B and H are directly shielded by the upstream interfering building. They exhibit less pressure magnitude due to reduction of velocity. This also affects the faces C and G as the magnitude of pressure also decreases on these faces. The size of vortices formed at the wake of the principal building decreases due to the presence of interfering buildings on both sides. The velocity near the wake region increases because of this phenomenon. As a result, the suction on the faces D, E and F decreases compared to isolated case.

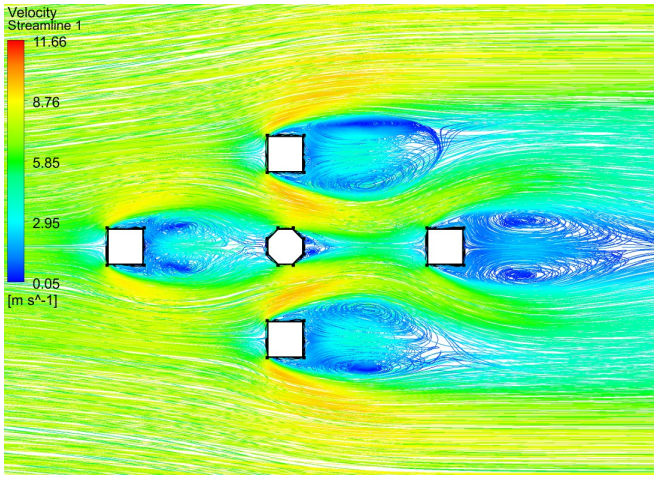

Fig. 4 The flow characteristics at the vicinity of the building setup at 0° wind incidence angle

4.1 Force Coefficient comparison

The force coefficients for the principal building can be defined as follows.

$$C_{fx,y} = \frac{F_{x,y}}{0.6V_z^2 A_{ex,y}} \quad (1)$$

Where C_{fx} is the mean drag coefficient, and C_{fy} is the mean lift coefficient. The drag coefficient variation with wind incidence angle is shown in Fig. 5. The drag coefficient is maximum at 0° wind incidence angle for both isolated and interfering cases. A remarkable variation between isolated and interfering case is noted at 0°, 15° and 45° wind angles. The most considerable difference in drag coefficients for both the cases is recorded as 40% at 45° wind incidence angle.

The variation of lift coefficient with the wind incidence angle for isolated and interference condition are displayed in Fig. 6. The change of lift coefficient with the wind incidence angle is shown in Fig. 6. The lift coefficient is maximum at 90° wind incidence angle for the isolated case, but for the interfering case, the peak value can be observed at 15° wind incidence angle. A remarkable variation between isolated and interfering case is noted at all the wind angles except for 0°. The most significant difference in lift coefficients for both the cases is observed as 100% at 90° wind incidence angle.

Both the drag coefficient and lift coefficient show significant deviation between isolated and interfering conditions with varying wind incidence angles. The lift coefficients especially show huge variation at different wind incidence angles. The designers would have to be exceptionally careful of adverse across-wind effect while designing the octagonal plan shaped building in these interfering conditions.

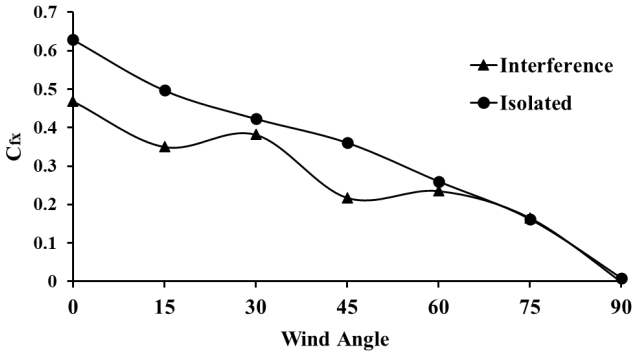

Fig. 5 The comparison of drag coefficients between the isolated and interfering condition

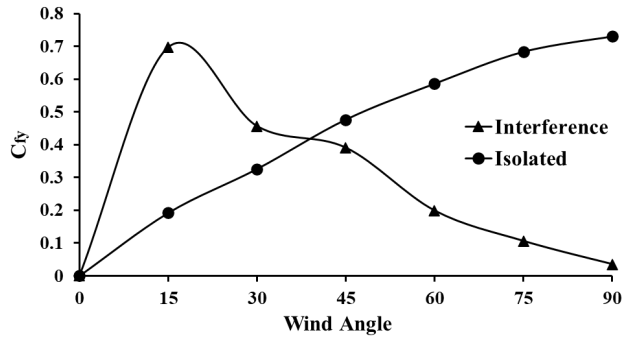

Fig. 6 The comparison of lift coefficients between the isolated and interfering condition

4.2 Pressure Coefficient comparison

The variation of pressure coefficient with wind incidence angles are for both interference, and isolated conditions are depicted in Fig. 7. The mean pressure coefficient for each face of the principal building can be defined as stated below.

$$C_p = \frac{\text{Avearage value of pressure in each face}}{0.6V_z^2} \quad (2)$$

A significant difference between interfering and isolated conditions can be noted for almost all the faces of the principal building. Among all the faces, the most amount of variation can be observed in the faces A, B, C, E and H. Whereas, the faces D and F exhibits the least amount of contrast between isolated and interfering conditions under various wind incidence angles. For face A, significant variation can be seen for all the wind angles except for 60° wind angle. This condition is derived from the presence of an interfering building in the direct upstream of the principal building. The maximum deviation is 200% at 30° wind incidence angle. For face B, the maximum difference can be noted for wind incidence angles 0°, 15° and 75°. The maximum difference observed is 187% at 15° wind incidence angles. In the case of face C, huge variation can be noted between isolated and interfering condition for all the cases except for the region of 15°-45° wind incidence angles. The highest variation is 199% at 60° wind incidence angle. Face D does not exhibit as much difference as other faces, since the decrease of velocity due to the upstream buildings is almost nullified by the channelling effect of the side interfering building. Nonetheless, the maximum deviation here is 40% at 15° wind incidence angle. The face E shows more variation than face D due to shrinking of the vortices caused by the presence of the two side interfering buildings. The highest deviation at face E is 76% at 90° wind incidence angle. The face F also shows a similar amount of deviation between isolated and interfering cases for similar reasons. The greatest deviation here is 56% at 75° wind incidence angle. Face G again shows a great difference between isolated and interference cases except for 45° to 60° wind incidence angle zone. The side interfering building in the vicinity causes this deviation. The highest difference here is 73% at 90° wind incidence angle. For face H, maximum variation can be seen in the 0°-45° wind incidence angle region. The maximum variation between isolated and interfering case is 102% at 15° wind incidence angle. Significant fluctuations can be observed for all the faces of the principal building due to the interference effect of the four buildings in the vicinity.

4.3 Comparison of Peak Pressure

The peak pressure coefficients for the different faces of the principal building is enumerated as follows.

$$C_{p(peak)} = \frac{\text{Avearage value of peak pressure in different face}}{0.6V_z^2} \quad (3)$$

The variation of peak and mean pressure coefficients for interference condition with wind incidence angles are shown in Fig. 8. The faces A, B, C, D and E are chosen as typical faces to illustrate the deviation of peak and mean pressures with varying wind angles. A vast difference can be observed for the faces A, B and C. Whereas, the magnitude of deviation is much less for faces D and E

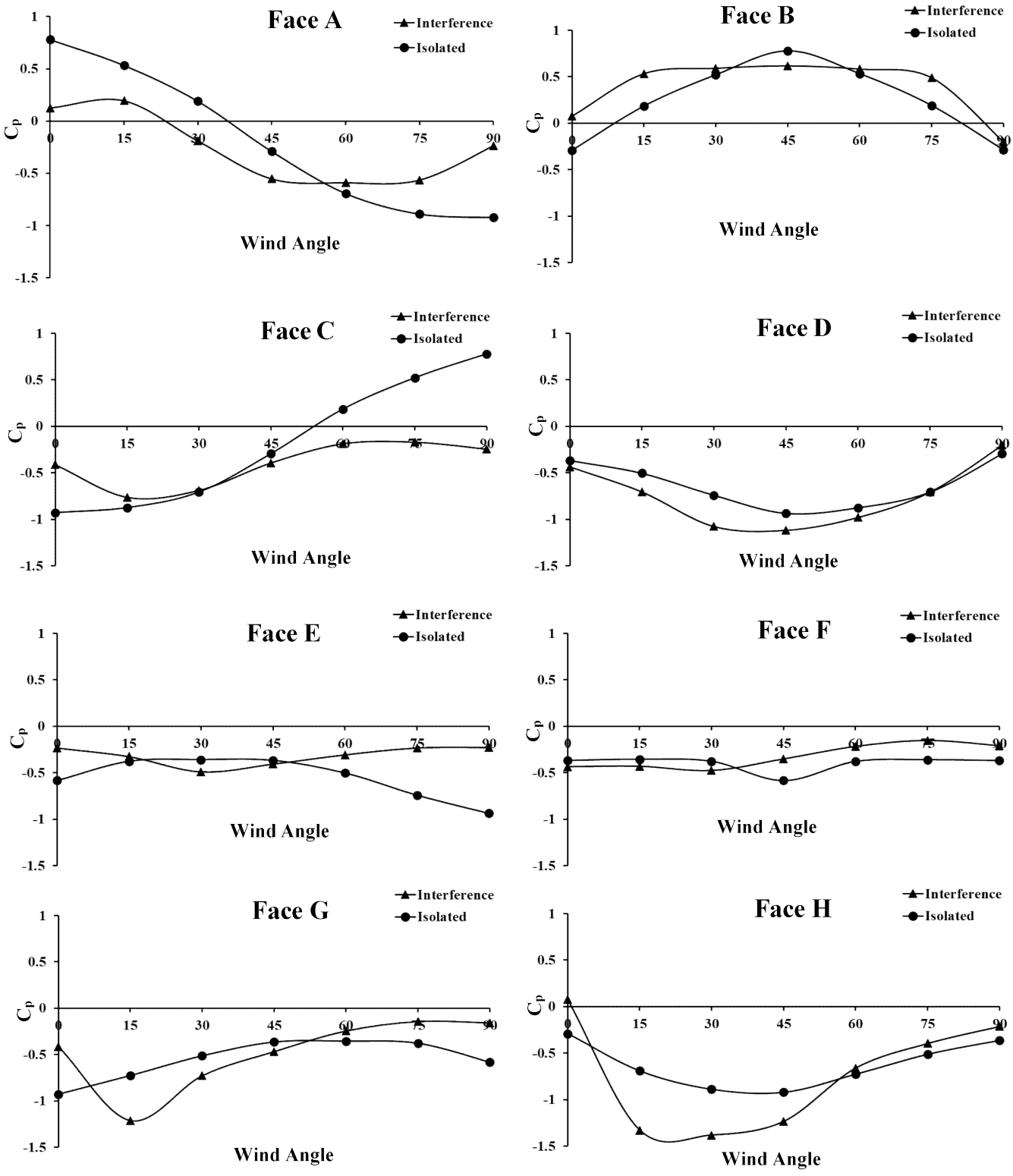

Fig. 7 The comparison of pressure coefficients between the isolated and interfering condition

.

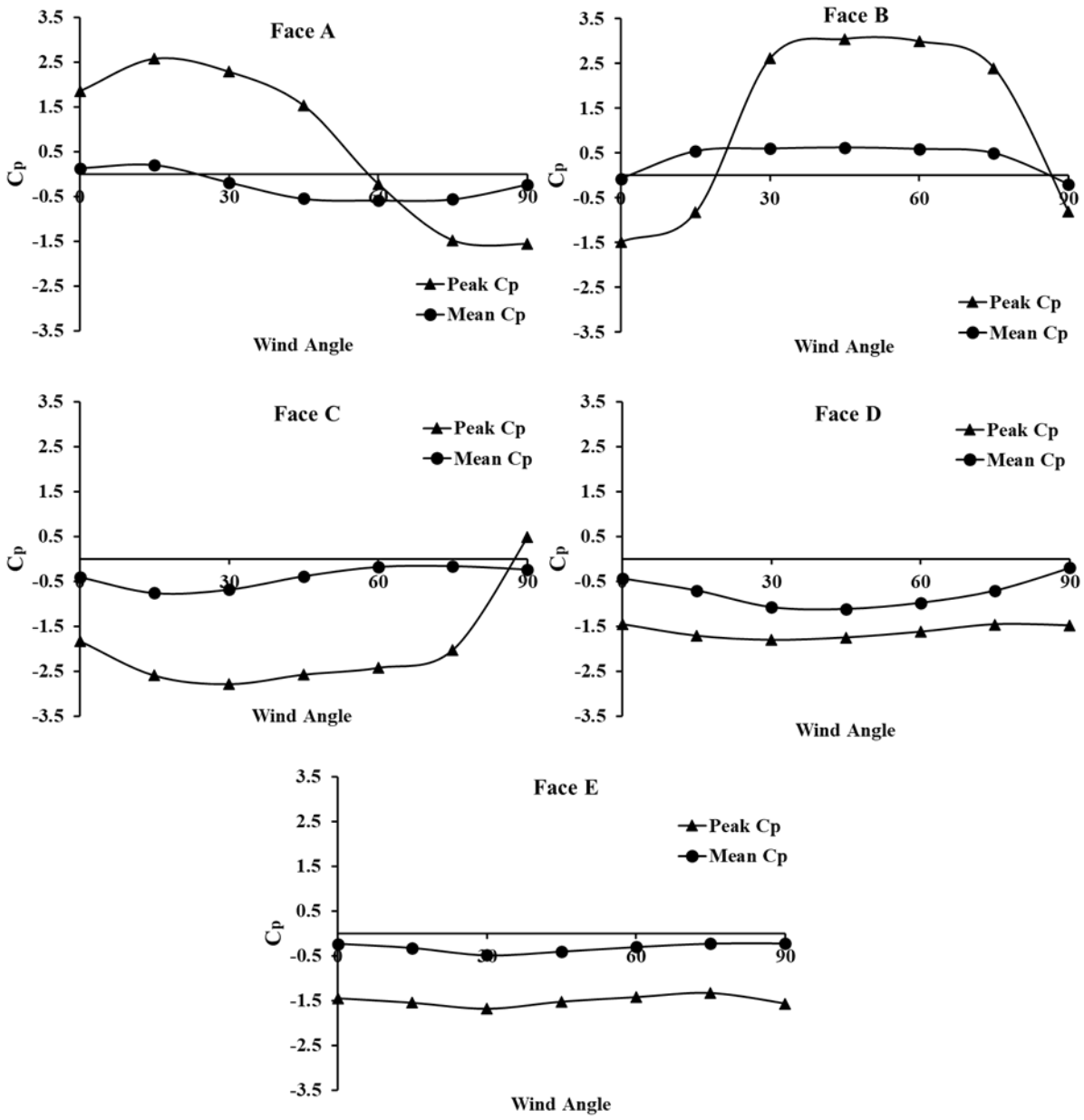

Fig. 8 The comparison of peak and mean pressure coefficients for the interfering condition with varying wind angles

4.3 Power Spectral Density of Pressure

The power spectral densities (PSD) of pressure are calculated on selected faces of the principal building for some typical wind angles. The PSDs are found out at points located at a distance of 10 mm from the side edge and top edge of each face. The modified PSD ($nS_p(n)/\sigma_p^2$) and reduced frequency (nD/U_H) are plotted against each other for these faces. Where, n=Frequency, $S_p(n)$=PSD of pressure, σ_p=Standard deviation of pressure varying with time at that point, D=cross-sectional dimension of the building, H=Height of the point from ground, U_H=mean wind velocity at height H.

The PSD plots at the selected points for 0° and 45° wind angles are depicted in Fig. 9 and Fig. 10 respectively. For 0° wind incidence angle, the Strouhal number remains same for both isolated and interfering conditions for the faces B, D and E. However, some discrepancies in the higher frequencies can be seen for interference case for all the faces. For 45° wind angle flattening of the PSD curve can be seen in interference condition for faces B, C and E. Though the vortices form at similar shedding frequencies, the power is less for the interference condition. So, weaker vortices are formed in cases of interference condition.

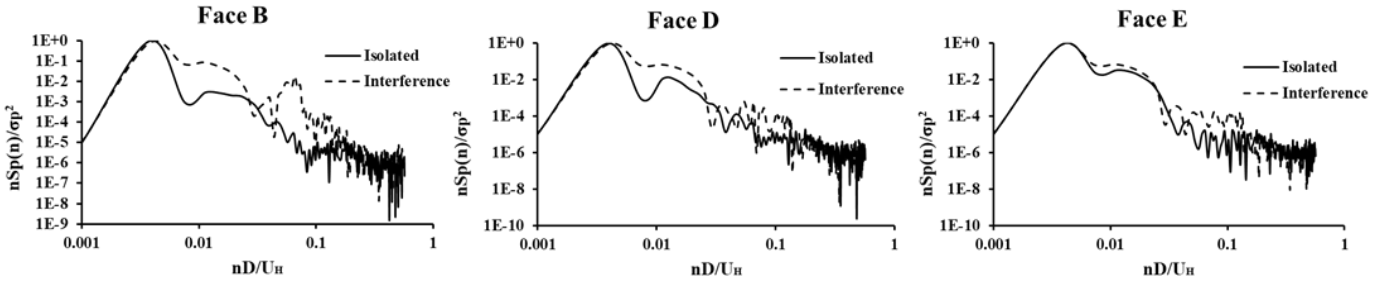

Fig. 9 The power spectral densities of pressure for the isolated and interfering condition at 0° wind angle

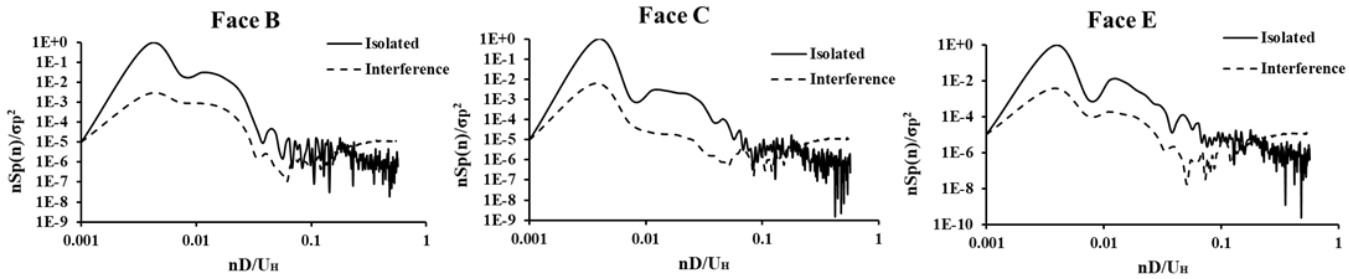

Fig. 10 The power spectral densities of pressure for the isolated and interfering condition at 45° wind angle

5. Conclusion

The drag coefficient and lift coefficient show a notable difference between isolated and interfering conditions. The lift coefficient exhibits a more significant variation than the drag coefficient. The across-wind effect is more prominent than the along-wind effect in the interfering conditions. The greatest deviation in drag coefficients for both the cases is noted as 40% at 45° wind incidence angle. Whereas for lift coefficient deviation for both the cases is observed as 100% at 90° wind incidence angle. The maximum value of the drag coefficient is at 0° wind angle for both isolated and interference condition. The lift coefficient, however, peaks at 30° wind angle for interference condition, while the isolated condition has its peak at 90° wind angle. The most deviation in pressure coefficients can be observed on faces A, B, C and H. The maximum variation is as high as 200% in some cases. The least amount of variation can be noted on faces D and F. In these cases, the maximum variation is only 56%. The disparity between mean and peak pressure is greatest on faces A, B and C. But faces D and E exhibits a relatively smaller deviation between mean and peak pressures. The pressure spectra show the minimum difference between isolated and interference condition for 0° wind angle. However, for 45° wind angle, the variation becomes significant. Here in interference condition, the vortices form at similar shedding frequencies compared to isolated condition, but the power is less. So, much smaller and weaker vortices are formed in the interference condition.

Disclosures

Free Access to this article is sponsored by SARL ALPHA CRISTO INDUSTRIAL.

References

1. Hui, Yi, Yukio Tamura, and Akihito Yoshida. 2012. “Mutual Interference Effects between Two High-Rise Building Models with Different Shapes on Local Peak Pressure Coefficients.” Journal of Wind Engineering and Industrial Aerodynamics 104–106: 98–108.
2. Hui, Yi, Akihito Yoshida, and Yukio Tamura. 2013. “Interference Effects between Two Rectangular-Section High-Rise Buildings on Local Peak Pressure Coefficients.” Journal of Fluids and Structures 37: 120–33.
3. Kar, Rony, and Sujit Kumar Dalui. 2016. “Wind Interference Effect on an Octagonal Plan Shaped Tall Building Due to Square Plan Shaped Tall Buildings.” International Journal of Advanced Structural Engineering 8(1): 73–86.
4. Kar, Rony, Sujit Kumar Dalui, and Soumya Bhattacharjya. 2019. “An Efficient Optimization Approach for Wind Interference Effect on Octagonal Tall Building.” Wind and Structures, An International Journal 28(2): 111–28.
5. Lo, Yuan-lung, and Yong Chul Kim. 2019. “Estimation of Wind-Induced Response on High-Rise Buildings Immersed in Interfered Flow.” Journal ofApplied Science and Engineering 22(3): 429–48.
6. Lo, Yuan Lung, Yong Chul Kim, and Akihito Yoshida. 2017. “Effects of Aerodynamic Modification Mechanisms on Interference from Neighboring Buildings.” Journal of Wind Engineering and Industrial Aerodynamics 168(December 2016): 271–87.

7. Menter, F. R. 1994. “Two-Equation Eddy-Viscosity Turbulence Models for Engineering Applications.” AIAA Journal 32(8): 1598–1605.

8. Sharma, Ashutosh, Hemant Mittal, and Ajay Gairola. 2019. “Aerodynamics of Tapered and Set-Back Buildings Using Detached-Eddy Simulation.” Wind and Structures, An International Journal 29(2): 111–27.

9. Sy, Long Doan, Hitoshi Yamada, and Hiroshi Katsuchi. 2019. “Interference Effects of Wind-over-Top Flow on High-Rise Buildings.” Journal of Wind Engineering and Industrial Aerodynamics 187(January): 85–96.

10. Yu, X. F., Z. N. Xie, J. B. Zhu, and M. Gu. 2015. “Interference Effects on Wind Pressure Distribution between Two High-Rise Buildings.” Journal of Wind Engineering and Industrial Aerodynamics 142: 188–97.

11. Yu, Xianfeng, Zhuangning Xie, and Ming Gu. 2018. “Interference Effects between Two Tall Buildings with Different Section Sizes on Wind-Induced Acceleration.” Journal of Wind Engineering and Industrial Aerodynamics 182(September): 16–26.